SL25

POLYMORPHS OF ARSENIC SULFIDE AND THEIR PROMISING ANTI-CANCER EFFECTS

A. Zorkovská[1], Z. Bujňáková[1], P. Baláž[1], J. Sedlák[2]

[1]*Institute of Geotechnics, Slovak Academy of Sciences, Watsonova 45, Košice, Slovakia*
[2]*Cancer Research Institute, Slovak Academy of Sciences, 833 91 Bratislava, Slovakia*
zorkovska@saske.sk

Keywords: realgar, pararealgar, milling, nanoparticles, anti-cancer effect

Abstract

Nanosuspensions of arsenic sulfide (As_4S_4) polymorphs (realgar and pararealgar) were prepared by circulation mill, with average particle size below 150 nm. The nanosuspensions were stable up to six weeks. Their anti-cancer effects were tested and compared on human lung cancer H460 cell line. Induction of DNA damage and increase of apoptotic cells was observed. The arsenic dissolution from the nanosuspensions in simulated gastric and intestinal fluids reached 12–13.5%.

Introduction

Arsenic sulfides have been utilized for a long time in the manufacture of cosmetics, foods, glass, insecticides, pigments, and in medicine as well [1]. In Western medicine, approximately 60 different arsenic preparations have been developed and used in pharmacological history. In traditional Chinese medicines different forms of mineral arsenicals are used, and realgar alone is included in 22 oral remedies, recognized by the Chinese Pharmacopeia Committee (2005). In the recent years its potential anticancer effects have been studied [2,3]. Production of nanocrystals is an approach to increase the drug solubility and its bioavailability. Here, the arsenic sulfides were prepared as nanosuspensions in circulation mill.

The As_4S_4 has at least three distinct polymorphs: i) the -As_4S_4 phase, with monoclinic crystal structure (space group $P2_1/n$), structurally identical to the mineral realgar, which is stable at room temperature, ii) the high temperature phase, -As_4S_4, with base-centered monoclinic crystal structure (space group C2/c) stable above 260 °C, which slowly reconverts to the -phase upon cooling, iii) and the monoclinic pararealgar (space group $P2_1/c$) bright yellow product formed upon exposure to visible light of both red and -phases [4]. There are two As–As covalent bonds and four As–S–As covalent bridges in the As_4S_4 subunits of both realgar (or -phase) and pararealgar. Transformation from realgar to pararealgar needs rearrangement of the molecular subunits involving As–S and As–As bond breaking.

Experimental

The investigation was carried out with mineral realgar – sample A, collected from Allchar locality (R. Macedonia) and pararealgar. The pararealgar was prepared innovately by milling – sample B (planetary mill Pulverisette 6, Fritzsch, Germany, sample weight 5 g, revolutions of the milling shaft 400 min^{-1}, milling time 60 min) or classically, by exposure of realgar to sunlight for 1 month – sample C. The preparation of the nanosuspensions was performed in a laboratory circulation mill MiniCer (Netzsch, Germany) in the presence of 300 mL of 0.5% polyvinylpyrrolidone (PVP) solution as nonionic stabilizer. PVP is one of the most used carriers for the preparation of nanosuspensions for medical application. The mill was loaded with yttrium stabilized ZrO_2 milling balls. After milling, the resulting nanoparticle suspensions were filtrated through a 0.22 m sterile filter.

X-ray diffraction measurements were carried out using a D8 Advance diffractometer (Bruker, Germany) equipped with a / goniometer, Cu K radiation (40 kV, 40 mA), secondary graphite monochromator, and scintillation detector. The diffraction data were collected over an angular range $10 < 2 < 100°$ with steps 0.03° and a counting time 20 s/step. The commercial Diffrac^{plus} Eva software has been used for phase analysis according to the ICDD - PDF2 database.

The particle size distribution was measured by photon cross-correlation spectroscopy using a Nanophox particle sizer (Sympatec, Germany).

Dissolution tests were conducted in simulated gastric fluid (SGF) composed of 0.2% NaCl in 0.7% HCl (pH = 1.3) and in a simulated intestinal fluid (SIF) composed of 0.042 % NaOH, 0.4 % $NaH_2PO_4.9H_2O$ and 0.6% NaCl with pH 6.5 at 36.5°C over a period of 240 minutes. The cytotoxicity on human lung cancer H460 was determined by colony forming assay. H460 cells were seeded onto 6-well plates with a density of 60 cells per well and incubated overnight. The cells were then treated with samples at various concentrations (0.156, 0.625, 1, 4, 16 and 64 g/ml). After incubation for 10 days the values of 50% inhibition concentration (IC_{50}) were determined. Cell cycle progression was monitored using DNA flow cytometry.

Results

Characterization of the materials

Realgar – sample A.

High-purity mineral, realgar, crystallizing in monoclinic crystal structure, space group $P2_1/n$, JCPDS 01-076-9449 (Fig. 1a).

Pararealgar – sample B and C, prepared by two alternative pathways:

B - Milling of realgar in a planetary mill Pulverisette 6. The XRD pattern of the sample after milling is shown on Fig.1c, the pararealgar- phase, crystallizing in the base

centered monoclinic system, space group C2/c, JCPDS 01-075-8666 was confirmed (Fig.1b). Line broadening and relative intensity decrease indicate the decrease of crystallite size and amorphization.

C - Irradiation of realgar by sunlight during one month. Absorption of visible photons with energies in the range 1.85–2.48 eV leads to irreversible isomerization of realgar to pararealgar, whereby the positions of one arsenic atom and one sulfur atom in the As_4S_4 cluster become exchanged [5], the process is accompanied by visible color change of the mineral from red to yellow. The transformation, realized by structural rearrangement and bond-breakings, leads also to considerable amorphization, as it can be seen from the XRD pattern on Fig. 1c. The product is a structurally non-homogeneous, multiphase system, with the main component pararealgar (monoclinic $P2_1/c$ phase, JCPDS 01-083-1013) and - phase. Non-transformed realgar can be also detected.

The nanosuspensions were prepared from samples A and C. The estimated average particle size x_{50} was 137 nm (142 nm) for the realgar (pararealgar) nanosuspensions, respectively, and 99% of particles were confirmed to be smaller than 200 nm. Interestingly, the main pararealgar component, present in the sample C, can not be detected in the obtained nanosuspension, which is composed of the majority pararealgar- phase and of some non-transformed realgar (Fig. 2).

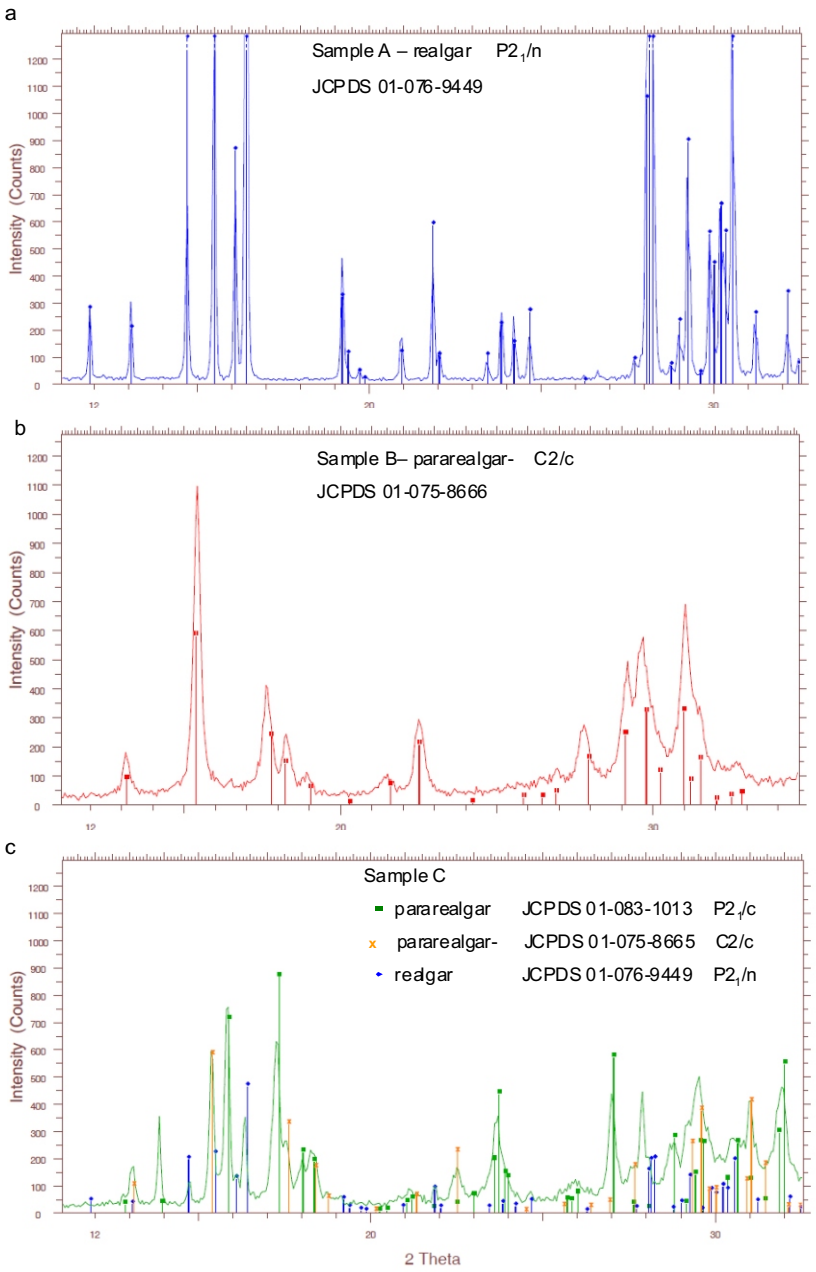

Figure 1. XRD patterns showing the phase composition of the source samples for preparation of nanosuspensions.

Dissolution in simulated gastric and intestinal fluids

Great rise in the solubility of arsenic was achieved by nanomilling, the amount of dissolved arsenic after 240 minutes of leaching in SGF + SIF increased from 2% to 12% (13.5%) for the nanomilled realgar (pararealgar), respectively. These results are very promising with respect to the published literature results. For comparison, only 0.6% of arsenic of the total realgar content was finally released into simulated gastric juice in [6], whereas some authors reported that 4% of arsenic from realgar were traced in gastric and intestinal fluids [7].

Anti-cancer effects

The nanomilled samples showed increased cytotoxicity. The values of 50% inhibition concentration (IC_{50}) of milled samples to H460 cells were 0.033 (0.031) g/mL for the nanomilled realgar (pararealgar). For comparison, this concentration for the used anti-cancer agent, cisplatin, is 0.01 g/mL. In general, the results imply that the lung cancer cells are susceptible to the treatment with these samples.

Cell cycle progression and induction of apoptotic cells

The H460 cells were treated with various concentrations of arsenic sulfides for 24, 48 and 72 h. The cell cycle distribution was determined, monitoring the G1 (growth phase), S (DNA replication phase) and G2/M (growth phase immediately preceding cell mitosis) phases.

The treatment of H460 cells with nanomilled A and C samples for 24 and 48 h resulted in reduction of G1 phase, accumulation of G2/M phase, and appearance of SubG1 cells (indicating apoptotic cells). Similarly to cisplatin, significantly increased number of SubG1 cells was observed after 72 h, indicating the cell cycle interference which may trigger the apoptotic pathways.

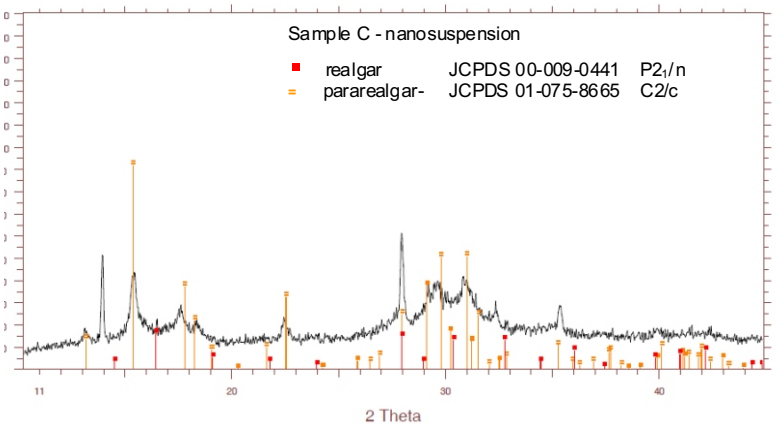

Figure 2. XRD pattern of the nanomilled sample C (light-irradiated realgar).

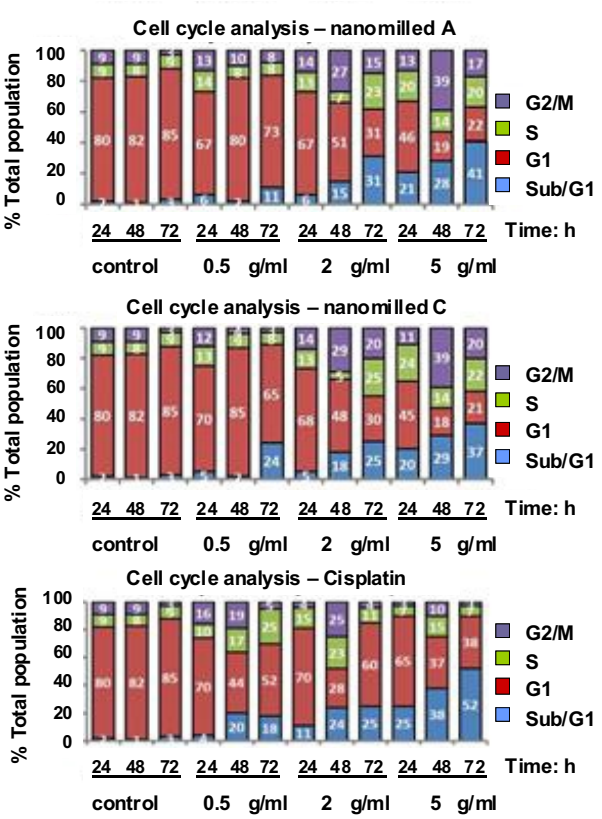

Figure 3. Cell cycle perturbation and apoptotic cell death induced by nanosuspensions prepared from samples A and C, and cisplatin for comparison.

Summary

Nanosuspensions of realgar and light irradiated realgar (composed of pararealgar, -phase and realgar) with average particle size below 150 nm were prepared in a circulation mill. The nanosuspensions were stable for more then one month. They have shown increased cytotoxicity and DNA damage activity on H460 lung cancer cells, with accumulation of G2/M phase inducing apoptotic cells.

References

1. R. Bentley, T.G. Chasteen, *J. Chem. Educ.* **7** (2002), 51.
2. Y. Tian, X. Wang, R. Xi, W. Pan, S. Jiang, Z. Li, Y. Zhao, G. Gao, D. Liu, *Int. J. Nanomed.* **9** (2014), 745.
3. P. Baláž, Z. Bujňáková, O. Kartachova, M. Fabián, B. Stalder, *Mater. Lett.* **104** (2013) 84.
4. L. Bindi, P. Bonazzi, *Am. Miner.* **92** (2007) 617.
5. P. Naumov, P. Makreski, G. Jovanovski, *Inorg. Chem.* **46** (2007) 10624.
6. S.Y. Kwan, S.K. Tsui, T.O. Man, *Anal. Lett.* **34** (2001) 1431.
7. J. Koch, S. Sylvester, V.W.M. Lai, A. Owen, K.J. Reimer, W.R. Cullen, *Toxicol. Appl. Pharm.* **222** (2007) 357.

Acknowledgements

The Slovak Grant Agency VEGA (2/0064/14 and 2/0027/14), the Agency for Science and Development (project APVV-0189-10) and the European Regional Development Fund (nanoCEXmat I and II - ITMS 26220120019 and 26220120035) are gratefully acknowledged.

SL26

The influence of the time od tooth development on microstructure of dental hydroxylapatite

ZÁVISLOST MIKROSTRUKTURY DENTÁLNÍHO HYDROXYLAPATITU NA DÉLCE VÝVOJE ZUBU

Anna Kallistová[1,2], Ivan Horáček[3], Roman Skála[1,2]

[1]Ústav geochemie, mineralogie a nerostných zdrojů, Přírodovědecká fakulta, Karlova Univerzita, Albertov 6, 128 43, Praha 2, Česká Republika, kallistova@gli.cas.cz
[2]Geologický ústav, AV CR, v.v.i., Rozvojová 269, 165 00, Praha 6, Česká Republika
[3]Katedra zoologie, Přírodovědecká fakulta, Karlova Univerzita, Viničná 7, 128 44, Praha 2, Česká Republika

Sklovina patří k nejvíce namáhaným anorganickým komponentám v tělech savců a významným způsobem ovlivňuje kvalitu a délku života jedince. Její odolnost závisí na vzájemném uspořádání agregátů hydroxylapatitových krystalitů (HAP) a jejich vlastnostech. Zatímco na organizaci agregátů se spolupodílí buněčná aktivita (ameloblasty), případně pre-existující organická matrice, vliv vlastností HAP na kvalitu skloviny nebyl doposud dostatečně zkoumán. Zde prezentovaná modelová studie se zabývá mikrostrukturou HAP molárů s rozdílnou délkou pre-eruptivního vývojového stádia u laboratorních miniprasat a její implikace pro výslednou kvalitu skloviny. Naše výsledky potvrzují, že délka pre-eruptivního stádia má pozitivní vliv na kvalitu skloviny, přičemž vliv mechanického opotřebení zubu na mikrostrukturu byl vyloučen.

SL27

STRUCTURE ANALYSIS OF NYLON 6 NANOFIBERS PREPARED BY NANOSPIDER TECHNOLOGY

A. Čajka[1], P. Čapková[1], J. Pavlík[1], M. Munzarová[2]

[1]Faculty of Science, J.E. Purkyně University, České mládeže 8, 40096 Ústí nad Labem
[2]Nanovia, s.r.o., Litvínov, Podkrušnohorská 271, 436 03 Litvínov-Chudeřín
Pavla.Capkova@ujep.cz

Polymer nanofibers find use in a wide range of areas such as: filtration [1], protective clothing, pharmaceuticals [2], tissue engineering [3], etc. The greatest attention of all polymeric fibers attracts nylon 6 due to its extraordinary properties: biodegradability, biocompatibility and good mechanical properties [4]. Various experimental arrangements and equipments have been described in literature for spinning of nylon 6 nanofibers either by melt spinning using extruder attached to a pump, see for example [5]) or by electrospinning with syringe attached to capillary tip connected to positive electrode [6]. Morphology and structure of the fibers prepared by these techniques has been characterized in dependence on spinning conditions and technology parameters [6,7]. However, the structure of fibers prepared by NANOSPIDER technology is less studied, although this technology is industrially used and for practice more significant. This study is devoted to the structure analysis of nylon 6 nanotextile prepared by NANOSPIDER technology under various conditions and for various technology parameters.

It is well known, that nylon 6 is polymorphic, having the following crystal structures: (1) The - form described by Brill [8] and Holmes et al. [9] and (2) the -form determined by Holmes et al. [9]. Both structures are monoclinic and differ from each other by arrangement of the polymeric chains, as one can see in figure 1. It is also known, that the melt spinning using extruder or electrospinning using capillary tip connected to positive electrode results in nylon 6 nanofibers composed of 3 structural phases: and amorphous part and their mutual proportion depends on spinning parameters. Phase composition of nylon 6 nanofibers prepared by nanospider technology has not been investigated. Present work deals with the effect of spinning distance (i.e. distance between nanospider electrodes) on the

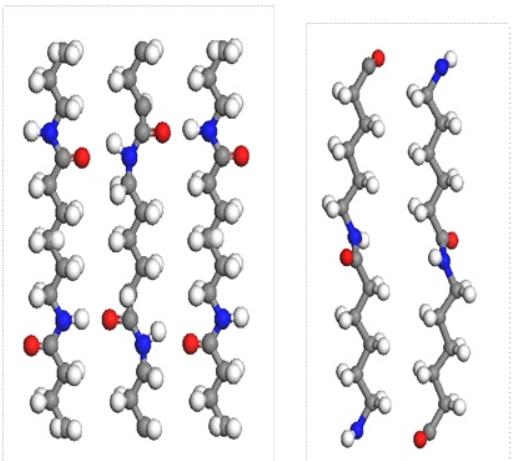

Figure 1: Arrangement of polymer chains in *ab* plane in crystal structure of -phase (left) and -phase (right).

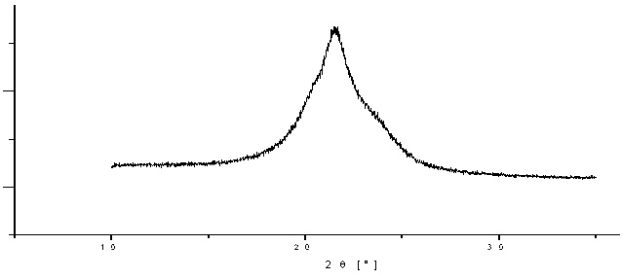

Figure 2. Diffraction profile of nylon 6 nanotextile prepared for spinning distance 15 cm (radiation CuK).

structure of nylon 6 nanofibers, prepared in laboratory nanospider typ NS Production Line NS 1 WSU.

Four nanotextile samples have been prepared for spinning distance: 150, 200, 250 and 300 mm. Wide angle X-ray scattering observable for all samples exhibits diffraction profile, which indicates the presence of and phase with a contribution of amorphous component. Example of such a profile is in the figure 2. Shoulders on the profile indicate the presence of -phase, while the central main peak corresponds to -phase. Large broadening shows a very poor crystallinity and the presence of amorphous phase.

Unraveling of the diffraction profiles for all spinning distances used in our experiment showed that:

- Increase of the spinning distance leads to higher degree of crystalinity, i.e. decrease of amorphous component and increase of crystallite size
- Increase of the spinning distance led also to the increased proportion of -phase in the sample.
- For all samples i.e. all spinning distances 150-300 mm, the nanotextile exhibits the strong texture, where the polymer fiber axis in $\langle 020 \rangle$ direction for both phases is preferentially oriented in the textile plane. The degree of preferred orientation within individual fibers can't be estimated.
- Crystallite size roughly estimated was 5 10 nm, while the average fiber diameter was 50 250 nm. Increasing spinning distance results in thinner fibers and in better homogeneity in fiber diameters and smaller number of failures having the shape of beads on fibers.

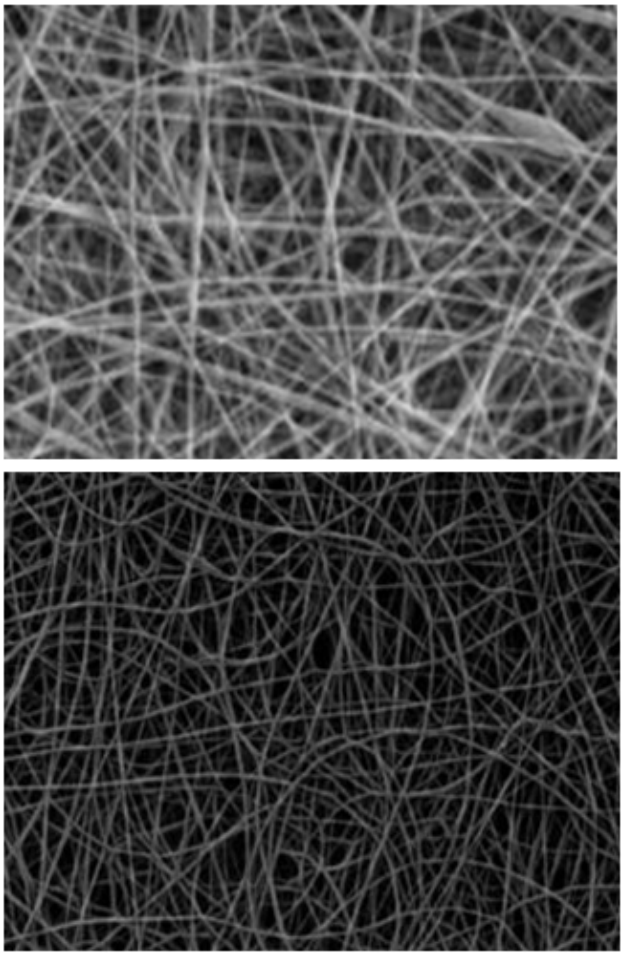

Figure 3. Nanotextiles prepared for spinning distance 150 mm (top) and 300 mm (bottom).

1. H. R. Ant M. P. Bajgai, Ch. Yi, R. Nirmala, K. T. Nam, W. Baek, H. Y. Kim., *Colloids and Surfaces A: Physicochemical and Engineering Aspects*. 370 (2010) 87-94.
2. P. Raghavan, X. Zhao, J. K. Kim, J. Manuel, G. S. Chauhan, J. H. Ahn, C. Nan., *Electrochim. Acta* 54 (2008) 228-234.
3. S. G. Kumbar, S. P. Nukavarapu, R. James, L. S. Nair, C. T. Laurencin, *Biomaterials* 29(2008) 4100-4107.
4. J. L. Pey*, Anti-Corros. Methods Matter*. 44 (1997) 94-99.
5. T. D. Fornes, D.R. Paul, *Polymer* 44 (2003) 3945-3961.
6. S. Zhang, W. S. Shim, J. Kim, *Materials* 30 (2009) 3659-3666.
7. S. S. A. Deyab, M. H. E. Newehy, R. Nirmala, A. A. Megeed, H. Y. Kim, *Korean Journal of Chemical Engineering*. 30 (2013) 422-428.
8. R. Brill, *Z physik Chem* B53(1943) 61-66.
9. R. Holmes, R; C.W. Bunn, D.L. Smith, *J Polym Sci* 17 (1955) 619-624.

SL28

STUDY OF HIGH TEMPERATURE PHASE OF TITANATE NANOTUBES

Tereza Brunátová[1], Zdeněk Matěj[1], Peter Oleynikov[2], Stanislav Daniš[1], Daniela Popelková[3], Radomír Kužel[1]

[1]Charles University, Faculty of Mathematics and Physics, Dept.of Condensed Matter Physics, Prague, Czech Republic
[2]Stockholm University, Dept. of Materials and Environmental Chemistry, Stockholm University, SE-106 91 Stockholm, Sweden
[3]Institute of Macromolecular Chemistry, Academy of Sciences of the Czech Republic, Prague, Czech Republic

Titanate nanotubes (Ti-NT) are very promising material with many possible applications in bionedicine, in solar cells, lithium batteries, fuel cells etc [1]. Their structure is not fully undertood and there exists several possible stuctures of Ti-NT [1]. The study of temperature stability of Ti-NT is important because some of possible applications of Ti-NT require heating [1]. By heating of Ti-NT titanate nanowires are obtained. Similarly to Ti-NT several possible phases of titanate nanowires can be discovered as for example: $Na_2Ti_6O_{13}$ [2], $Na_2Ti_3O_7$ [2], rutile phase of TiO_2 [2-4], anatase phase of TiO_2 [2], [3], beta TiO_2 [4]. The final structure depends also on the amount of sodium ions if some are present in original Ti-NT sample.

In this contribution, the structure of Ti-NT will be briefly introduced and mainly the structure of titanate nanorods and titania nanowires will be discused. The study of titanate nanorods was done by combination of powder X-ray diffraction and 3D rotation electron diffraction. The titanate nanorods were prepared by heating of titanate nanotubes up to 850 °C. The structure of final product at 850 C depends on heating conditions and time of heating. We studied samples - heated in air and in vacuum. The heating in air were done in following way: firstly the sample was heated at 850 C for 105 minutes and for 1000 minutes, the last heating was at 900 C for 1000 minutes. The heating in vacuum was don similar way: firstly heated at 850 C for 105 minutes and 3000 minutes, then at 900 C for 3000 minutes and last heating was at 1000 C for 3000 minutes. Differences between samples heated in air and vacuum are that in air is observed sodium hexatitanate, anatase and rutile but sample heated in vacuum has only visible diffraction lines from anatase witch afterwards transform to rutile.

1. Bavykin DF. V.,Walsh F. C.: Titanate and titania nanotubes, synthesis, properties and application, RSC Publishing, 2010.
2. Morgado E., jr, de Abreu M. A. S., Pravia O. R. C., Marinkovic B. A., Jardim P. M., Rizzo R.C., Araujo A.S.: A study on the structure and thermal stability of titanate nanotubes as a function of sodium content, Solid State Science, 8, 2006.
3. Yu J., Yu H., Cheng B., Trapalis C.: Effects of calcination temperature on the microstructures and photocatalytic activity of titanate nanotubes, Journal of Molecular Catalysis A, 249, 2006.
4. Suzuki Y., Yoshikawa S.: Synthesis and thermal analysis of TiO_2-deriveted nanotubes prepared by the hydrotherma method, Jounal Material Res., 19, 2004.